

A two-dimensional array of single-hole quantum dots

Van Riggelen, F.; Hendrickx, N. W.; Lawrie, W. I.L.; Russ, M.; Sammak, A.; Scappucci, G.; Veldhorst, M.

DOI

[10.1063/5.0037330](https://doi.org/10.1063/5.0037330)

Publication date

2021

Document Version

Final published version

Published in

Applied Physics Letters

Citation (APA)

Van Riggelen, F., Hendrickx, N. W., Lawrie, W. I. L., Russ, M., Sammak, A., Scappucci, G., & Veldhorst, M. (2021). A two-dimensional array of single-hole quantum dots. *Applied Physics Letters*, 118(4), Article 044002. <https://doi.org/10.1063/5.0037330>

Important note

To cite this publication, please use the final published version (if applicable).
Please check the document version above.

Copyright

Other than for strictly personal use, it is not permitted to download, forward or distribute the text or part of it, without the consent of the author(s) and/or copyright holder(s), unless the work is under an open content license such as Creative Commons.

Takedown policy

Please contact us and provide details if you believe this document breaches copyrights.
We will remove access to the work immediately and investigate your claim.


A two-dimensional array of single-hole quantum dots ^F

Cite as: Appl. Phys. Lett. **118**, 044002 (2021); <https://doi.org/10.1063/5.0037330>

Submitted: 12 November 2020 . Accepted: 10 December 2020 . Published Online: 27 January 2021

 F. van Riggelen,  N. W. Hendrickx,  W. I. L. Lawrie,  M. Russ,  A. Sammak,  G. Scappucci, and  M. Veldhorst

COLLECTIONS

 This paper was selected as Featured



View Online



Export Citation



CrossMark

ARTICLES YOU MAY BE INTERESTED IN

Conditioning nano-LEDs in arrays by laser-micro-annealing: The key to their performance improvement

Applied Physics Letters **118**, 043101 (2021); <https://doi.org/10.1063/5.0038070>

Exceeding 400% tunnel magnetoresistance at room temperature in epitaxial Fe/MgO/Fe(001) spin-valve-type magnetic tunnel junctions

Applied Physics Letters **118**, 042411 (2021); <https://doi.org/10.1063/5.0037972>

How good are 2D transistors? An application-specific benchmarking study

Applied Physics Letters **118**, 030501 (2021); <https://doi.org/10.1063/5.0029712>



Your Qubits. Measured.

Meet the next generation of quantum analyzers

- Readout for up to 64 qubits
- Operation at up to 8.5 GHz, mixer-calibration-free
- Signal optimization with minimal latency

Find out more

 Zurich Instruments

A two-dimensional array of single-hole quantum dots

Cite as: Appl. Phys. Lett. **118**, 044002 (2021); doi: [10.1063/5.0037330](https://doi.org/10.1063/5.0037330)

Submitted: 12 November 2020 · Accepted: 10 December 2020 ·

Published Online: 27 January 2021




View Online



Export Citation



CrossMark

F. van Riggelen,¹  N. W. Hendrickx,¹  W. I. L. Lawrie,¹  M. Russ,¹  A. Sammak,²  G. Scappucci,¹ 
and M. Veldhorst^{1,a)} 

AFFILIATIONS

¹QuTech and Kavli Institute of Nanoscience, Delft University of Technology, Lorentzweg 1, 2628 CJ Delft, The Netherlands

²QuTech and Netherlands Organization for Applied Scientific Research (TNO), Stieltjesweg 1, 2628 CK Delft, The Netherlands

^{a)} Author to whom correspondence should be addressed: m.veldhorst@tudelft.nl

ABSTRACT

Quantum dots fabricated using methods compatible with semiconductor manufacturing are promising for quantum information processing. In order to fully utilize the potential of this platform, scaling quantum dot arrays along two dimensions is a key step. Here, we demonstrate a two-dimensional quantum dot array where each quantum dot is tuned to single-charge occupancy, verified by simultaneous measurements using two integrated radio frequency charge sensors. We achieve this by using planar germanium quantum dots with low disorder and a small effective mass, allowing the incorporation of dedicated barrier gates to control the coupling of the quantum dots. We measure the hole charge filling spectrum and show that we can tune single-hole quantum dots from isolated quantum dots to strongly exchange coupled quantum dots. These results motivate the use of planar germanium quantum dots as building blocks for quantum simulation and computation.

Published under license by AIP Publishing. <https://doi.org/10.1063/5.0037330>

Quantum information requires qubits that can be coherently controlled and coupled in a scalable manner,¹ while quantum error correction and scalable interconnects strongly benefit from the ability to couple qubits along at least two dimensions.^{2,3} Across all the different qubit technologies, quantum dots⁴ fabricated using techniques compatible with standard semiconductor manufacturing are particularly promising.⁵ Furthermore, realizing two-dimensional quantum dot arrays may allow us to construct highly scalable qubit tiles such as crossbar arrays⁶ supporting quantum error correction⁷ for fault-tolerant quantum computation.

A key challenge is, therefore, to develop two-dimensional arrays of quantum dots that exhibit a high level of uniformity and long quantum coherence and that can be operated with excellent control. Initial research centered around low-disorder gallium arsenide (GaAs) heterostructures,^{8,9} which advanced to exciting demonstrations such as coherent spin transfer across an array of quantum dots¹⁰ and the operation of a two-dimensional quantum dot array.¹¹ Nonetheless, group III–V materials suffer from hyperfine interaction, resulting in fast spin dephasing and reduced operation fidelity. Instead, group IV materials can be isotopically enriched^{12,13} to virtually eliminate dephasing due to a nuclear spin bath. This has stimulated research on silicon and led to several orders of magnitude improvement in coherence times.^{14,15} While advances in devices based on silicon heterostructures have led to the operation of linear arrays containing up to nine quantum dots,¹⁶ the

relatively large effective mass of silicon electrons, the presence of valley energy states, and the finite disorder complicates progress.¹⁷ Although fabrication is advancing to complementary metal-oxide-semiconductor (CMOS) foundry-manufactured devices,^{18,19} demonstrations on two-dimensional quantum dot arrays have been limited to reaching single-electron occupancy in up to three dots within a 2×2 array.^{20–23} Reaching simultaneously the single-charge regime with all quantum dots in a two-dimensional array fabricated using CMOS foundry compatible materials remains, thereby, an outstanding challenge.

Germanium is rapidly emerging as an alternative material to realize spin qubits²⁴ since holes in germanium have favorable properties such as a small effective mass,²⁵ large excited-state energies due to the absence of valley degenerate states,²⁶ and strong spin–orbit coupling for electrically driven single-qubit rotations without the need for external components.^{27–29} High-quality Ge/Si core-shell nanowires enabled the construction of a triple quantum dot in a linear arrangement, albeit only in the multi-hole regime.³⁰ The realization of high-quality strained Ge/SiGe quantum wells³¹ has led to the development of quantum dots,^{32,33} demonstration of long hole spin relaxation times,³⁴ and the operation of a single-hole qubit³⁵ and enabled the execution of two-qubit logic in germanium.³⁶ Furthermore, quantum dots in planar germanium are realized using industry compatible techniques,³⁷ promising large-scale implementations provided that germanium quantum dots can be engineered beyond linear arrangements.

Here, we realize a two-dimensional quantum dot array using materials compatible with existing CMOS technology and demonstrate a quadruple germanium quantum dot. We obtain excellent control over the charge occupancy and the interdot coupling. The device consists of the quantum dot grid and an additional two quantum dots on the sides that are used for radio frequency (rf) charge sensing. We are able to tune each quantum dot to the single-hole occupancy, and we find shell filling as is expected for a circular quantum dot with spin degeneracy. This demonstrates a qubit state manifold with large separation energy since excited states, such as valley energy states, are absent. We exploit the integrated barrier gates to gain independent control over the hole occupancy and the tunnel coupling between neighboring quantum dots. We use this to demonstrate the single-hole occupancy in the full quadruple quantum dot array as a stepping stone toward two-dimensional arrays of quantum dot qubits.

Figure 1(a) shows a scanning electron microscopy (SEM) image of the quantum dot grid, and Fig. 1(b) shows a schematic image of the potential landscape and the control gates of the quantum dot system. Fabrication is based on a multilayer gate design³³ and described in the [supplementary material](#), Sec. I. Holes in strained germanium benefit from a low effective mass, low disorder, and the absence of valley states. These assets ease constraints in fabrication and the quantum dot design, which makes it possible to define a 2×2 quantum dot grid with only two overlapping gate electrodes. The quantum dots are defined using plunger gates P and are coupled through barrier gates B. We have fabricated the barrier gates as the first layer and the plunger gates as the second layer, which results in a good addressability of both the tunnel couplings and quantum dot energy levels. The aluminum Ohmics serve as hole reservoirs for the charge sensors. Controllable loading of the quantum dots is obtained through an additional barrier gate between the sensor and the quantum dots (B_{S1} and B_{S2}). The charge occupation in the dots is measured with the nearby sensing

dots. We use rf reflectometry to achieve a high measurement bandwidth of the sensor impedance, which allows for measuring charge stability diagrams in real time.

Figure 2(a) shows a charge stability diagram corresponding to quantum dot pair Q_1 – Q_3 . See the [supplementary material](#), Sec. II for the stability diagram corresponding to quantum dot pair Q_2 – Q_4 . In this measurement, we preserve the sensitivity of the sensor, by offsetting the effect of a change in voltage on the plunger gate of the quantum dots with a small change in voltage on the plunger gate of the sensors. From the linear charge addition lines in Fig. 2(a), we infer that the capacitive coupling between the plunger gate and the neighboring quantum dot is small and does not require compensation. In Fig. 2(b), we show the addition energies for each of the four quantum dots in the few-hole regime. We define the addition energy as the energy required for adding an extra hole to the quantum dot. The addition energies are extracted from the charge stability diagrams, by analyzing the spacing between the addition lines for all the dots. The change in gate voltage is converted into energy, using a lever arm $\alpha = 0.19$ eV/V. Steps are observed for hole occupations $N = 2$ and $N = 6$, which are consistent with shell filling for a circular quantum dot and considering the spin degree of freedom.^{38,39} These experiments also highlight the absence of low-energy excited states such as valley states, which would give rise to a different shell filling pattern.⁴⁰ It is interesting to observe that quantum dot Q_1 and Q_4 show shell filling as expected for circular quantum dots, while for Q_2 and Q_3 , the expected peaks in addition energy are less pronounced. Moreover, Q_2 and Q_3 show an increased addition energy for $N = 4$. We ascribe this difference to Q_2 and Q_3 being positioned close to the sensor quantum dots, which are operated using relatively large negative potentials. The electric field from the sensors might distort the circular potential to a more elliptical shape, which would, in turn, modify the electronic structure and cause an increased addition energy at half-filling.⁴¹

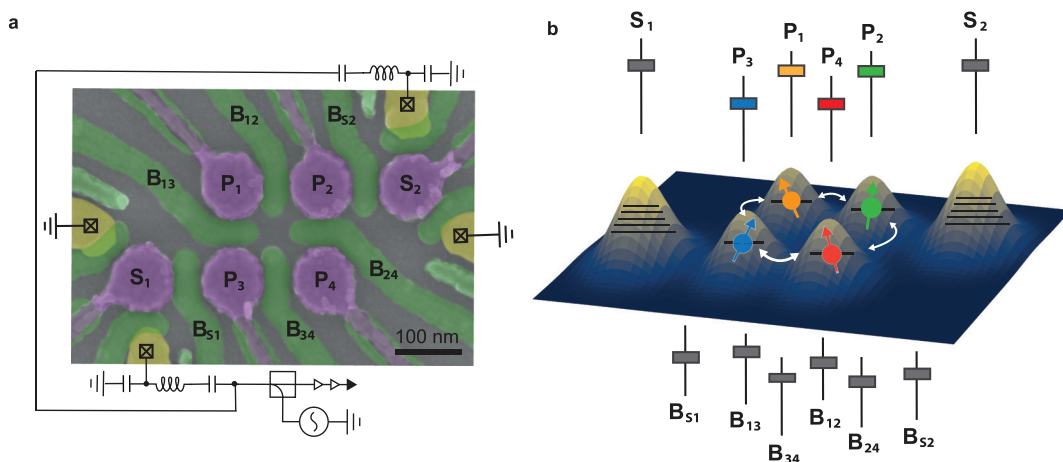


FIG. 1. A 2×2 germanium quantum dot grid with two integrated rf sensors. (a) False colored SEM image of a sample similar to the one on which the measurements are performed. The plunger gates of the quantum dots P are colored in purple, the barrier gates B are colored in green, and the aluminum Ohmics in yellow, which serve both as the source and drain contacts for rf sensing, as well as charge reservoirs for the quantum dots. (b) Schematic representation of the potential landscape, illustrating how the plunger and barrier gates control the quantum dots. In the image, each quantum dot is occupied with a single hole ($N = 1$), which is color coded per quantum dot (yellow for Q_1 , green for Q_2 , blue for Q_3 , and red for Q_4). The charge occupation in a quantum dot is controlled by a plunger gate, symbolized by a slider above the image with the same color. The sensing dots are tuned into the multi-hole regime, illustrated by the many energy levels drawn in the quantum dot. The coupling between the quantum dots, indicated by the arrows, is controlled by a barrier gate, depicted by a slider below the image.

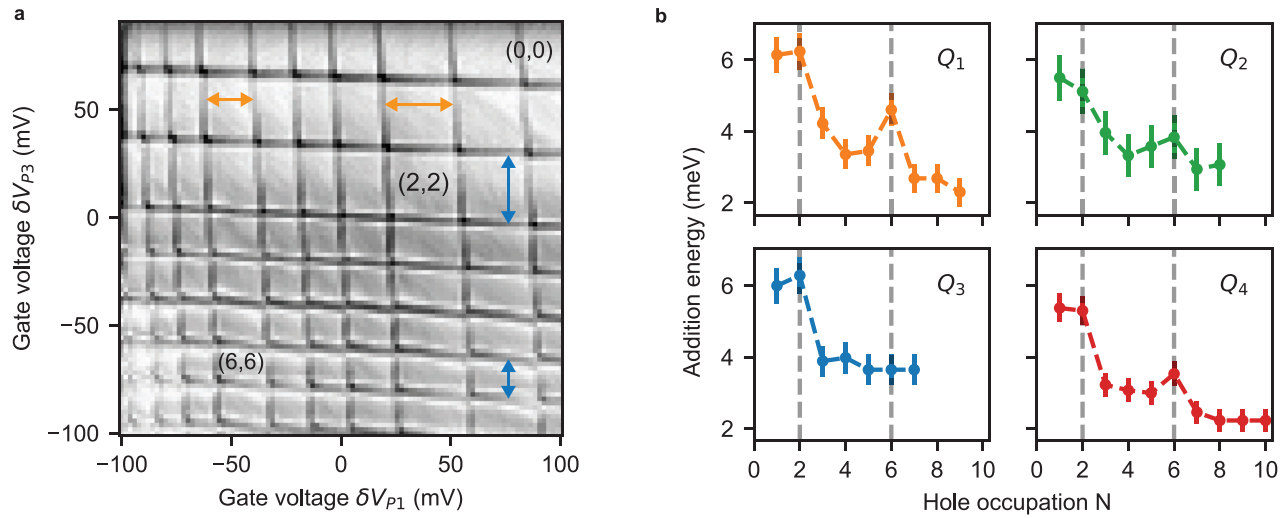


FIG. 2. Charge filling in the individual quantum dots. (a) A charge stability diagram of the double quantum dot Q_1 – Q_3 with negligible tunnel coupling (see the [supplementary material](#), Sec. II for the quantum dot pair Q_2 – Q_4). Here, the results are shown as measured with sensor S_1 , the sensor closest to the quantum dot pair. We can observe all transitions with both sensors, albeit with reduced sensitivity for the more remote quantum dots, as shown in [Fig. 4](#). The hole occupation (N_{Q1} , N_{Q3}) is indicated in the charge stability diagram. (b) Addition energy for the four quantum dots, extracted from the corresponding stability diagrams and converted using a lever arm $\alpha = 0.19$ eV/V. The dashed gray lines correspond to the hole fillings for which increased addition energy is expected due to shell filling when considering a circular potential landscape and spin degeneracy [also indicated by orange and blue arrows in (a) for Q_1 and Q_3 , respectively].

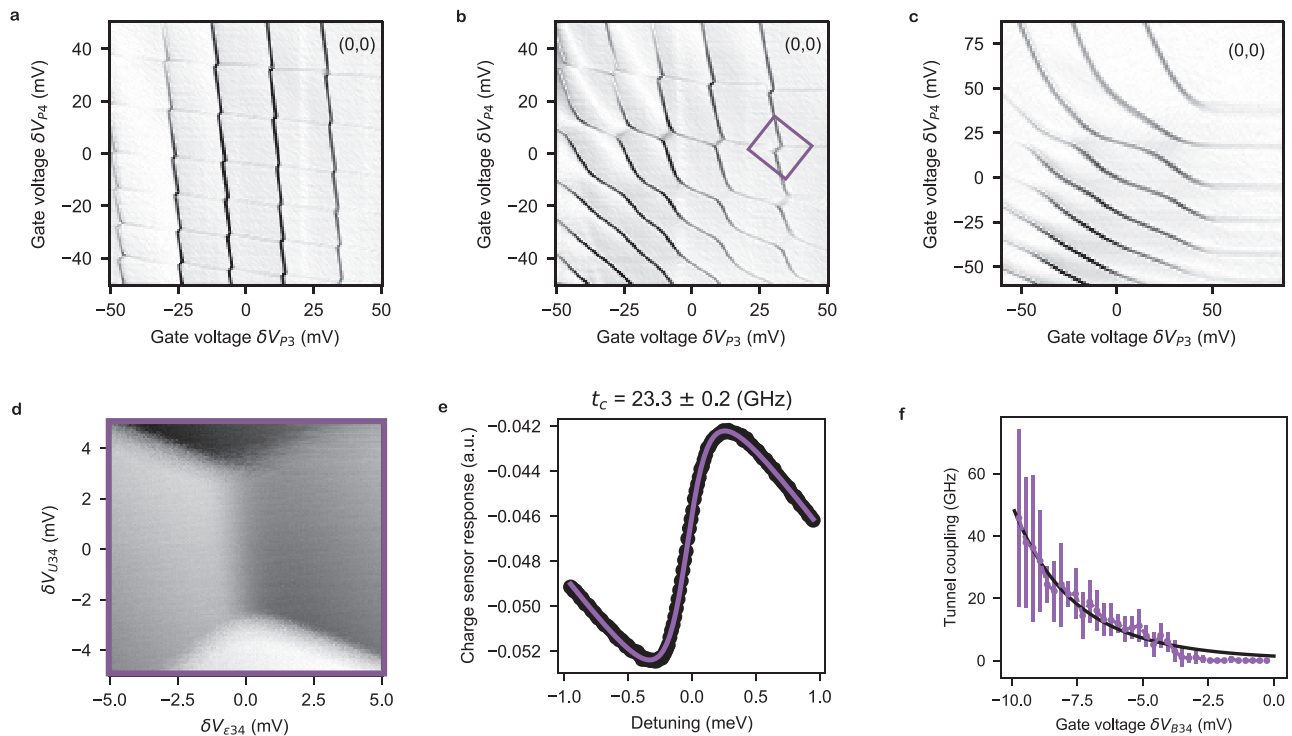


FIG. 3. Controllable interdot tunnel coupling. (a)–(c) Charge stability diagram for quantum dot pair Q_3 – Q_4 with barrier gate voltage $V_{B34} = -1010.6$ mV (a), $V_{B34} = -1055.1$ mV (b), and $V_{B34} = -1137.1$ mV (c). By varying the barrier gate voltage, we can freely tune the tunnel coupling over a large range. (d) Zoom-in on the relevant $(1,1)$ – $(0,2)$ charge configuration where we quantify the tunnel coupling. (e) By fitting the charge polarization line,⁴² we obtain the tunnel coupling, which is $t_c = 23.3 \pm 0.2$ GHz. (f) By varying the gate voltage V_{B34} , we can control the tunnel coupling up to 40 GHz. Reduced charge sensor sensitivity for higher tunnel coupling causes the uncertainty in the measurement to increase. The trend of the tunnel coupling corresponds well to a fit based on the WKB theory (see the [supplementary material](#), Sec. V for further details).

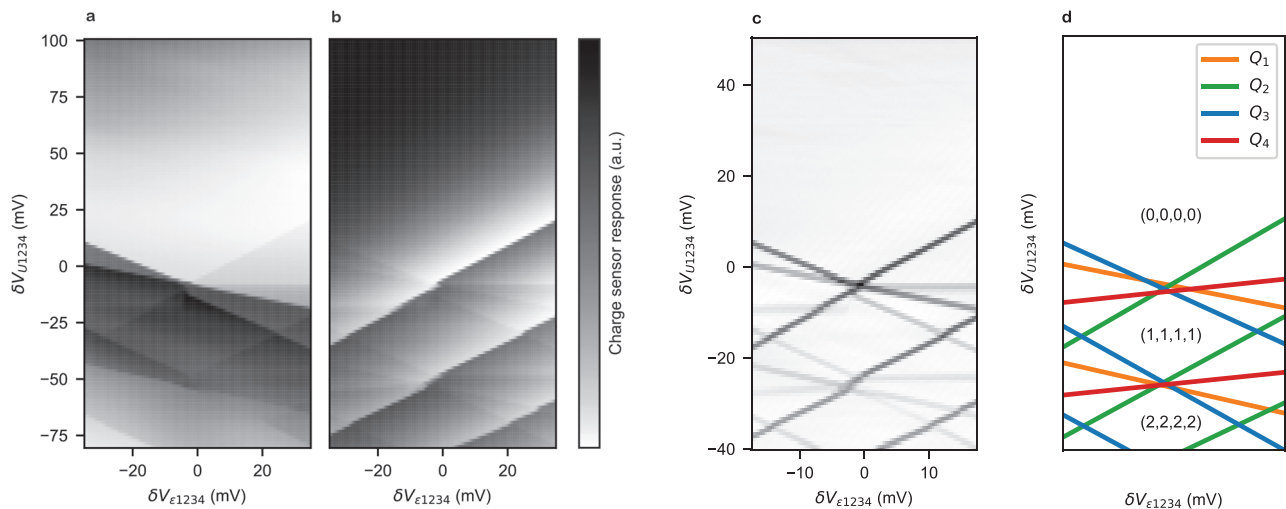


FIG. 4. Quadruple quantum dot in germanium. (a) and (b) Charge stability diagram of the four quantum dot system, obtained by simultaneous readout of S_1 and S_2 . (a) Charge sensor response of sensor S_1 . (b) Charge sensor response of S_2 . While we can observe all transitions with each sensor, we observe a significant larger sensitivity to the quantum dots neighboring the sensor. (c) Derivative of the combined response signal, clearly revealing the charge addition lines for each of the quantum dots. (d) Schematic representation explaining the charge addition lines as measured in (c), confirming the absence of additional lines from spurious quantum dots or traps and demonstrating a single-hole quadruple quantum dot array. Hole occupation in the dots ($N_{Q1}, N_{Q2}, N_{Q3}, N_{Q4}$) is indicated for an empty system, single-hole occupation, and double hole occupation for all four dots.

Having shown control over the hole occupation of the individual quantum dots, we focus on the interdot tunnel coupling. Figures 3(a)–3(c) show charge stability diagrams of a double quantum dot defined by plunger gates P_3 and P_4 for different barrier gate potentials, compensating the effect of the change in voltage on the sensor. We find that we can tune the quantum dots from being fully isolated, to a strongly coupled regime, and to merging quantum dots, indicating a high level of tunability. Importantly, we reach all regimes while freely choosing the hole occupancy.

To quantify the tunnel coupling between the quantum dots, we analyze the charge polarization lines. Figure 3(d) shows the anticrossing corresponding to the $(1, 1) \rightarrow (0, 2)$ charge configurations. We measure the charge sensor response along the detuning axis and determine the tunnel coupling by fitting the charge polarization lines,⁴² as shown in Fig. 3(e). By changing the barrier gate voltage, we can control the tunnel coupling and find that we can tune the interdot tunnel coupling over a range from completely off to beyond 40 GHz. Note that we can set larger tunnel couplings [see, for example, Fig. 3(c)]. However, in this regime, we are not able to make reliable fittings of the charge polarization line, due to the reduced charge sensitivity of the sensor, as a result of the merging of Q_3 and Q_4 .

After focusing on the interdot coupling, we now show that we can form a quadruple quantum dot in the 2×2 array, reaching single-hole occupation for all four quantum dots simultaneously. With both sensors, we can detect charge transitions of each quantum dot within the array although a significantly stronger sensitivity is obtained for the quantum dots neighboring the sensor. In order to conveniently tune and demonstrate the single-hole occupation for all quantum dots, a virtual gate set is defined (see the supplementary material, Sec. III) such that the addition lines of all four dots have a distinctive slope. In Figs. 4(a) and 4(b), we show the charge stability diagram as measured

by the individual charge sensors. Taking the derivative of the signal and summing them result in Fig. 4(c). The observed charge addition lines are shown in Fig. 4(d).

In conclusion, we have demonstrated shell filling, tunable interdot coupling, and the tuning of a quadruple quantum dot to the single-hole states. The shell filling experiments underscore the high quality of planar germanium quantum dots as a platform for spin qubits. Moreover, this statement is supported by the demonstration that the tunnel coupling between single holes can be tuned over a large range, from isolated quantum dots to strongly coupled and merging quantum dots. This tunability is promising for quantum simulation with quantum dots such as simulating metal–insulator transitions.⁴³ Simultaneously, the ability to turn the exchange interaction on and off is highly advantageous for digital quantum computation and can be used to program two-qubit logic at their sweet spots. The demonstration of a quadruple quantum dot positioned in a two-dimensional array is an important stepping stone toward quantum information processing using standard semiconductor manufacturing.

See the supplementary material for a description of the device fabrication (Sec. I), the charge stability diagram of $Q_2 - Q_4$ (Sec. II), the definition of the virtual gates (Sec. III), a short description on how the lever arm was obtained (Sec. IV), and the model that was fitted to tunnel coupling data shown in Fig. 3(f).

We thank Caroline Smulders and all the members of the Veldhorst group for inspiring discussions. M.V. acknowledges support through projectruimte and Vidi grants, associated with the Netherlands Organization of Scientific Research (NWO).

The authors declare no competing interest.

DATA AVAILABILITY

The data that support the findings of this study are openly available in 4TU.ResearchData at <https://doi.org/10.4121/13416488.v1>, Ref. 44.

REFERENCES

- ¹D. P. DiVincenzo, "The physical implementation of quantum computation," *Prog. Phys.* **48**, 771–783 (2000).
- ²B. Terhal, "Quantum error correction for quantum memories," *Rev. Mod. Phys.* **87**, 307 (2015).
- ³D. P. Franke, J. S. Clarke, L. M. K. Vandersypen, and M. Veldhorst, "Rent's rule and extensibility in quantum computing," *Microprocessors Microsyst.* **67**, 1–7 (2019).
- ⁴D. Loss and D. P. DiVincenzo, "Quantum computation with quantum dots," *Phys. Rev. A* **57**, 120–126 (1998).
- ⁵L. M. K. Vandersypen, H. Bluhm, J. S. Clarke, A. S. Dzurak, R. Ishihara, A. Morello, D. J. Reilly, L. R. Schreiber, and M. Veldhorst, "Interfacing spin qubits in quantum dots and donors—hot, dense, and coherent," *npj Quantum Inf.* **3**, 34 (2017).
- ⁶R. Li, L. Petit, D. P. Franke, J. P. Dehollain, J. Helsen, M. Steudtner, N. K. Thomas, Z. R. Yoskovits, K. J. Singh, S. Wehner, L. M. Vandersypen, J. S. Clarke, and M. Veldhorst, "A crossbar network for silicon quantum dot qubits," *Sci. Adv.* **4**, eaar3960 (2018).
- ⁷J. Helsen, M. Steudtner, M. Veldhorst, and S. Wehner, "Quantum error correction in crossbar architectures," *Quantum Sci. Technol.* **3**, 035005 (2018).
- ⁸J. R. Petta, A. C. Johnson, J. M. Taylor, E. A. Laird, A. Yacoby, M. D. Lukin, C. M. Marcus, M. P. Hanson, and A. C. Gossard, "Coherent manipulation of electron spins in semiconductor quantum dots," *Science* **309**, 2180–2184 (2005).
- ⁹F. H. Koppens, C. Buizert, K. J. Tielrooij, I. T. Vink, K. C. Nowack, T. Meunier, L. P. Kouwenhoven, and L. M. Vandersypen, "Driven coherent oscillations of a single electron spin in a quantum dot," *Nature* **442**, 766–771 (2006).
- ¹⁰Y. P. Kandel, H. Qiao, S. Fallahi, G. C. Gardner, M. J. Manfra, and J. M. Nichol, "Coherent spin-state transfer via Heisenberg exchange," *Nature* **573**, 553–557 (2019).
- ¹¹U. Mukhopadhyay, J. P. Dehollain, C. Reichl, W. Wegscheider, and L. M. K. Vandersypen, "A 2×2 quantum dot array with controllable inter-quantum dot tunnel couplings," *Appl. Phys. Lett.* **112**, 183505 (2018).
- ¹²K. Itoh, E. E. Haller, W. L. Hansen, J. W. Farmer, V. I. Ozhogin, A. Rudnev, and A. Tikhomirov, "High purity isotopically enriched 70 Ge and 74 Ge single crystals: Isotope separation, growth, and properties," *J. Mater. Res.* **8**, 1341–1347 (1993).
- ¹³K. M. Itoh and H. Watanabe, "Isotope engineering of silicon and diamond for quantum computing and sensing applications," *MRS Commun.* **4**(4), 143–157 (2014).
- ¹⁴M. Veldhorst, J. C. Hwang, C. H. Yang, A. W. Leenstra, B. De Ronde, J. P. Dehollain, J. T. Muhonen, F. E. Hudson, K. M. Itoh, A. Morello, and A. S. Dzurak, "An addressable quantum dot qubit with fault-tolerant control-fidelity," *Nat. Nanotechnol.* **9**, 981–985 (2014).
- ¹⁵J. T. Muhonen, J. P. Dehollain, A. Laucht, F. E. Hudson, R. Kalra, T. Sekiguchi, K. M. Kohei, D. N. Jamieson, J. C. McCallum, A. S. Dzurak, and A. Morello, "Storing quantum information for 30 seconds in a nanoelectronic device," *Nat. Nanotechnol.* **9**, 986–991 (2014).
- ¹⁶D. M. Zajac, T. M. Hazard, X. Mi, E. Nielsen, and J. R. Petta, "Scalable gate architecture for a one-dimensional array of semiconductor quantum dots," *Phys. Rev. Appl.* **6**, 054013 (2016).
- ¹⁷F. A. Zwanenburg, A. S. Dzurak, A. Morello, M. Y. Simmons, L. C. L. Hollenberg, G. Klimeck, S. Rogge, S. N. Coppersmith, and M. A. Eriksson, "Silicon quantum electronics," *Rev. Mod. Phys.* **85**, 961 (2013).
- ¹⁸R. Maurand, X. Jehl, D. Kotekar-Patil, A. Corna, H. Bohuslavskiy, R. Lavieville, L. Hutin, S. Barraud, M. Vinet, M. Sanquer, and S. De Franceschi, "A CMOS silicon spin qubit," *Nat. Commun.* **7**, 13575 (2016).
- ¹⁹R. Pillarisetty, N. Thomas, H. C. George, K. Singh, J. Roberts, L. Lampert, P. Amin, T. F. Watson, G. Zheng, J. Torres *et al.*, "Qubit device integration using advanced semiconductor manufacturing process technology," in IEEE International Electron Devices Meeting (IEDM) (2018), pp. 3–6.
- ²⁰F. Ansaloni, A. Chatterjee, H. Bohuslavskiy, B. Bertrand, L. Hutin, M. Vinet, and F. Kuemmeth, "Single-electron control in a foundry-fabricated two-dimensional qubit array," *arXiv:2004.00894* (2020).
- ²¹E. Chanrion, D. J. Niegemann, B. Bertrand, C. Spence, B. Jadot, J. Li, P. A. Mortemousque, L. Hutin, R. Maurand, X. Jehl *et al.*, "Charge detection in an array of CMOS quantum dots," *Phys. Rev. Appl.* **14**, 024066 (2020).
- ²²W. Gilbert, A. Saraiva, W. H. Lim, C. H. Yang, A. Laucht, B. Bertrand, N. Rambal, L. Hutin, C. C. Escott, M. Vinet, and A. S. Dzurak, "Single-electron operation of a silicon-CMOS 2×2 quantum dot array with integrated charge sensing," *Nano Lett.* **20**(11), 7882–7888 (2020).
- ²³J. Duan, M. A. Fogarty, J. Williams, L. Hutin, M. Vinet, and J. J. L. Morton, "Remote capacitive sensing in two-dimension quantum-dot arrays," *Nano Lett.* **20**(10), 7123–7128 (2020).
- ²⁴G. Scappucci, C. Kloeffer, F. A. Zwanenburg, D. Loss, M. Myronov, J.-J. Zhang, S. De Franceschi, G. Katsaros, and M. Veldhorst, "The germanium quantum information route," *Nat. Rev. Mater.* (published online, 2020).
- ²⁵M. Lodari, A. Tosato, D. Sabbagh, M. A. Schubert, G. Capellini, A. Sammak, M. Veldhorst, and G. Scappucci, "Light effective hole mass in undoped Ge/SiGe quantum wells," *Phys. Rev. B* **100**, 041304 (2019).
- ²⁶P. Stano, C. Hsu, L. C. Camenzind, L. Yu, D. Zumb, and D. Loss, "Orbital effects of a strong in-plane magnetic field on a gate-defined quantum dot," *Phys. Rev. B* **99**, 085308 (2019).
- ²⁷D. V. Bulaev and D. Loss, "Spin relaxation and decoherence of holes in quantum dots," *Phys. Rev. Lett.* **95**, 076805 (2005).
- ²⁸D. V. Bulaev and D. Loss, "Electric dipole spin resonance for heavy holes in quantum dots," *Phys. Rev. Lett.* **98**, 097202 (2007).
- ²⁹H. Watzinger, J. Kukučka, L. Vukušić, F. Gao, T. Wang, F. Schäffler, J. J. Zhang, and G. Katsaros, "A germanium hole spin qubit," *Nat. Commun.* **9**, 3902 (2018).
- ³⁰F. N. M. Froning, M. K. Rehmann, J. Ridderbos, M. Brauns, F. A. Zwanenburg, E. P. A. M. Bakkers, D. M. Zumbuhl, and F. R. Braakman, "Single, double, and triple quantum dots in Ge/Si nanowires," *Appl. Phys. Lett.* **113**, 073102 (2018).
- ³¹A. Sammak, D. Sabbagh, N. W. Hendrickx, M. Lodari, B. Paquelet Wuetz, A. Tosato, L. R. Yeoh, M. Bollani, M. Virgilio, M. A. Schubert, P. Zaumseil, G. Capellini, M. Veldhorst, and G. Scappucci, "Shallow and undoped germanium quantum wells: A playground for spin and hybrid quantum technology," *Adv. Funct. Mater.* **29**, 1807613 (2019).
- ³²N. W. Hendrickx, D. P. Franke, A. Sammak, M. Kouwenhoven, D. Sabbagh, L. Yeoh, R. Li, M. L. Tagliaferri, M. Virgilio, G. Capellini, G. Scappucci, and M. Veldhorst, "Gate-controlled quantum dots and superconductivity in planar germanium," *Nat. Commun.* **9**, 2835 (2018).
- ³³W. I. L. Lawrie, H. G. J. Eenink, N. W. Hendrickx, J. M. Boter, L. Petit, S. V. Amitonov, M. Lodari, B. Paquelet Wuetz, C. Volk, S. Philips *et al.*, "Quantum dot arrays in silicon and germanium," *Appl. Phys. Lett.* **116**, 080501 (2020).
- ³⁴W. I. L. Lawrie, N. W. Hendrickx, F. Van Riggelen, M. Russ, L. Petit, A. Sammak, G. Scappucci, and M. Veldhorst, "Spin relaxation benchmark and individual qubit addressability for holes in quantum dots," *Nano Lett.* **20**(10), 7237–7242 (2020).
- ³⁵N. W. Hendrickx, W. I. L. Lawrie, L. Petit, A. Sammak, G. Scappucci, and M. Veldhorst, "A single-hole spin qubit," *Nat. Commun.* **11**, 3478 (2020).
- ³⁶N. W. Hendrickx, D. P. Franke, A. Sammak, G. Scappucci, and M. Veldhorst, "Fast two-qubit logic with holes in germanium," *Nature* **577**, 487–491 (2020).
- ³⁷R. Pillarisetty, "Academic and industry research progress in germanium nano-devices," *Nature* **479**, 324–328 (2011).
- ³⁸S. Tarucha, D. G. Austing, T. Honda, R. J. van der Hage, and L. P. Kouwenhoven, "Shell filling and spin effects in a few electron quantum dot," *Phys. Rev. Lett.* **77**, 3613 (1996).
- ³⁹S. D. Liles, R. Li, C. H. Yang, F. E. Hudson, M. Veldhorst, A. S. Dzurak, and A. R. Hamilton, "Spin and orbital structure of the first six holes in a silicon metal-oxide-semiconductor quantum dot," *Nat. Commun.* **9**, 3255 (2018).
- ⁴⁰W. H. Lim, C. H. Yang, F. A. Zwanenburg, and A. S. Dzurak, "Spin filling of valley-orbit states in a silicon quantum dot," *Nanotechnology* **22**, 335704 (2011).
- ⁴¹S. M. Reimann and M. Manninen, "Electronic structure of quantum dots," *Rev. Mod. Phys.* **74**, 1283 (2002).

- ⁴²L. DiCarlo, H. J. Lynch, A. C. Johnson, L. I. Childress, K. Crockett, C. M. Marcus, M. P. Hanson, and A. C. Gossard, "Differential charge sensing and charge delocalization in a tunable double quantum dot," *Phys. Rev. Lett.* **92**, 226801 (2004).
- ⁴³T. Hensgens, T. Fujita, L. Janssen, X. Li, C. J. Van Diepen, C. Reichl, W. Wegscheider, S. Das Sarma, and L. M. Vandersypen, "Quantum simulation of a Fermi-Hubbard model using a semiconductor quantum dot array," *Nature* **548**, 70–73 (2017).
- ⁴⁴F. van Riggelen, N. Hendrickx, W. Lawrie, M. F. Russ, A. Sammak, G. Scappucci, and M. Veldhorst (2021). "Data accompanying the publication: A two-dimensional array of single-hole quantum dots," 4TU.ResearchData. <https://doi.org/10.4121/13416488.v1>.